Global exposure risk of frogs to increasing environmental dryness

Nicholas C. Wu[1,*], Rafael Parelli Bovo[2,3], Urtzi Enriquez-Urzelai[4], Susana Clusella-Trullas[5], Michael R. Kearney[6], Carlos A. Navas[2,7], Jacinta D. Kong[8,9]

[1]*Hawkesbury Institute for the Environment, Western Sydney University, New South Wales 2753, Australia*

[2]*Departmento de Fisiologia, Instituto de Biociências, Universidade de São Paulo, São Paulo 05508090, Brazil*

[3]*Department of Evolution, Ecology, and Organismal Biology, University of California Riverside, CA, United States*

[4]*Czech Academy of Sciences, Institute of Vertebrate Biology, Květná 8, 60365 Brno, Czech Republic*

[5]*Department of Botany and Zoology & School for Climate Studies, Stellenbosch University, Stellenbosch 7600, South Africa*

[6]*School of BioSciences, The University of Melbourne, Melbourne, Victoria, Australia*

[7]*Edward Bass Distinguished Scholar, YIBS/Ecology & Evolutionary Biology, Yale University, CT, United States*

[8]*School of Natural Sciences, Trinity College Dublin, Dublin 2, Ireland*

[9]*Department of Biology, Carleton University, Ottawa K1S 5B6, Canada*

[*]Corresponding author

Email: nicholas.wu.nz@gmail.com

ORCID: NCW (0000-0002-7130-1279), RPB (0000-0003-4345-6430), UEU (0000-0001-5958-2250), SCT (0000-0002-8891-3597), MRK (0000-0002-3349-8744), CAN (0000-0002-9859-0568), JDK (0000-0002-1085-8612)

Author contribution: NCW and CAN conceived the study, NCW and JDK compiled the data, RPB, CAN, and SCT provided additional unpublished data for 39 species, MRK developed the model and UEU developed the model simulations, NCW analysed the data, produced the figures, and wrote the initial draft. All authors contributed to the revisions.

Acknowledgement: This paper is dedicated to the late Professor Phillip J. Bishop (1957–2021) who was at the forefront of amphibian conservation research in the southern hemisphere. Phil dedicated more than 30 years to amphibian conservation and this study was inspired partly by his research and his passion for amphibians at the Word Congress of Herpetology in Dunedin, New Zealand, 2020.

Competing interests: The authors declare no competing interests.

Funding information: UEU is financially supported by the Institute of Vertebrate Biology of the Czech Academy of Sciences (RVO: 68081766), RPB received financial support by the São Paulo Research Foundation—FAPESP (#10/20061-6, #14/05624-5, #17/10338-0, #19/04637-0). SCT's amphibian research was supported by the National Research Foundation of South Africa.

Data accessibility: Data and code to reproduce the study are available on the GitHub repository: https://github.com/nicholaswunz/global-frog-drought and will be available on Zenodo upon acceptance.

ABSTRACT

Species exposed to prolonged drying are at risk of population declines or extinctions. A key missing element for assessments of climate change risk is the sensitivity of species to water loss and their microhabitat preference, or ecotype, as both dictate the risk of environmental drying. Here, we identified globally where water-sensitive ectotherms, i.e. anurans, are at risk to increasing aridity and drought, examined which ecotypes are more sensitive to water loss from 238 species, and estimated how behavioural activity is impacted by future drought and warming scenarios through biophysical models. Under an intermediate and high emission scenario, 6.6 and 33.5% of areas occupied by anurans will increase to arid-like conditions, and 15.4 and 36.1% are at risk of exposure to a combination of increasing drought intensity, frequency, and duration by 2080–2100, respectively. Critically, increasing arid-like conditions will increase water loss rates and anurans in dry regions will almost double the water loss rates under a high emission scenario. Biophysical models showed that during the warmest quarter of the year, the combination of drought and warming reduced an anuran's potential activity by 17.9% relative to the current conditions compared to warming alone which reduced potential activity by 8%. Our results exemplify the widespread exposure risk of environmental drying for anurans, posing a serious challenge for the lives of water-sensitive species beyond the effects of temperature alone.

Keywords: amphibian decline, climate change, dehydration, desiccation, hydroregulation, macrophysiology, thermoregulation

INTRODUCTION

Global warming and land modification are expected to increase the frequency and intensity of droughts, which are anomalous periods of low precipitation (Slette et al., 2019; Pokhrel et al., 2021; Zhao and Dai, 2022). This synergistic interaction is accelerating extinction risk for species sensitive to rapid water loss (Zylstra et al., 2019; Lowe et al., 2021). Amphibians are prime examples of terrestrial species that are heavily dependent on water, and often have higher rates of water turnover than other terrestrial animals (Lillywhite, 2006; Hillman et al., 2009). The group is characterised by their sensitivity to both environmental temperature and moisture. Thus, negative or challenging water balances can reduce opportunities for foraging, finding mates, and dispersal (Sodhi et al., 2008; Ficetola and Maiorano, 2016; Lertzman-Lepofsky et al., 2020). Despite synthesis studies on the effects of climate change on amphibians (Li et al., 2013; Campbell Grant et al., 2020), global assessments of climate vulnerability have mainly been through the lens of temperature (Snyder and Weathers, 1975; Gunderson and Stillman, 2015; Murali et al., 2023; Pottier et al., 2024b). Yet, the impact of extreme moisture deficit events such as drought, needs to be assessed, given the

sensitivity of amphibians to water loss and their threatened status relative to other taxonomic groups (Luedtke et al., 2023).

Assessing species vulnerability to climate change relies on the degree of environmental exposure and the species' sensitivity to the exposure (Williams et al., 2008). The extent of **exposure** to drying is mainly influenced by the frequency, intensity, and duration of the stressor. However, the impact of climate change is not singular (Rozen-Rechels et al., 2019). While environmental water stress primarily depends on surrounding water availability (in the air, substrate, and water bodies) and how much is evaporated or transpired by plants (Trenberth et al., 2014), warming alone will increase evaporation rates by increasing the vapor pressure deficit (VPD). VPD is one of the primary forces driving evaporation rates and atmospheric drought (Park Williams et al., 2013). High VPDs are known to be major drivers of mortality events in plants (Eamus et al., 2013; Grossiord et al., 2020), and the rise in evaporation rates reduces activity in many ectotherms (Kearney et al., 2018; Lertzman-Lepofsky et al., 2020) and increases exposure to lethal dehydration events in birds and mammals (Kearney et al., 2016; Albright et al., 2017; Iknayan and Beissinger, 2018). Experimental and field studies have suggested amphibians behaviourally prefer environments that maintain hydration over thermoregulation, emphasising the importance of water availability in informing climate vulnerability (Navas et al., 2007; Anderson and Andrade, 2017; Galindo et al., 2018). Understanding the water loss vulnerability is therefore a necessary component for determining species vulnerability to global environmental change.

Behavioural and physiological **sensitivity** to water loss can vary by species. Some ecological types ('ecotypes') have unique adaptations to drying conditions (Toledo and Jared, 1993). For example, fossorial species living in arid regions burrow underground during the non-breeding period to aestivate (Carvalho et al., 2010), and some are able to create water-proof cocoons to conserve water (Withers, 1995; Tracy et al., 2007). In contrast, some arboreal anurans produce skin waxy secretions that reduce evaporative water loss (Shoemaker and McClanahan, 1980; Stinner and Shoemaker, 1987; Amey and Grigg, 1995). Most amphibians, however, are vulnerable to dehydrating conditions compared to other terrestrial vertebrates and must therefore behaviourally maintain water balance by using shade, burrows, or by adopting a water conserving postures when inactive (Pough et al., 1983). Because of this diversity in natural history, some ecotypes are likely to be more sensitive to environmental drying than others due to the microclimate preferences and limited physiological adaptations to conserve water. The increased frequency and intensity of drought conditions—even for arid specialists—can impact anurans by restricting the activity periods for foraging, seeking mates, dispersing, and delaying breeding cycles (Wassens et

al., 2013), all of which ultimately affects population dynamics, disease susceptibility, and shifts in geographic distribution (Kohli et al., 2019; Zylstra et al., 2019; Kupferberg et al., 2022).

In this study, we aimed to (i) identify regions where anurans are at risk to increased aridity and drought by quantifying the spatial overlap between anuran species richness and areas of increasing aridification and drought (including intensity, frequency and duration) under future warming scenarios, (ii) examine ecotype sensitivity of adult anurans to evaporative water loss and water uptake through comparative meta-analyses, and (iii) simulate physiological limits for activity of a hypothetical adult frog in relation to future drought and warming scenarios in order to assess the relative effects of warming and/or drought on changes in potential activity hours for each water-conserving strategy under different climate scenarios. We focused on water loss risk for adult terrestrial anurans because most larval stages are aquatic and rely on water bodies.

METHODS

Aridity and drought risk

Global climatic water balance data

The global water cycle is complex, and many indices have been used to understand and predict environmental water stress across space and time (Spinoni et al., 2020; Ukkola et al., 2020; Li et al., 2021). Here, we used two common metrices of environmental dryness, the aridity index (AI), and the Palmer Drought Severity Index (PDSI). The AI represented the degree of dryness of the climate and is calculated as the ratio of the total amount of water supply (precipitation) relative to the amount of water loss (potential evapotranspiration). More arid regions have a smaller index value (Cherlet et al., 2018). In this study, the AI represented the broadscale dryness experienced by amphibians in that area. The PDSI is a widely used meteorological drought index calculated using soil moisture and precipitation data of previous months. By using surface air temperature and a physical water balance model, the PDSI takes into account the basic effect of global warming through potential evapotranspiration and is effective in determining long-term drought (Palmer, 1965; Dai et al., 2004). In this study, the PDSI represented extreme changes in meteorological water deficit or surplus experienced. The AI was categorised to five categories (Humid, Dry sub-humid, Semi-arid, Arid, and Hyper-arid) and the PDSI was categorised to seven categories (Extremely moist, Very moist, Moderate moist, Normal, Moderate drought, Severe drought, and Extreme drought) based on descriptions from Budyko (1961) and Palmer (1965) in **Table S1**.

High resolution (~4km^2) global data on precipitation (mm/month) and potential evapotranspiration (mm/month) were obtained from Abatzoglou et al. (2018) under 1) the current climate (1970–2000), 2) an intermediate greenhouse gas emission scenario of +2°C (Shared

Socioeconomic Pathway 2–4.5; SPP2–4.5), and 3) a high greenhouse gas emission or "business-as-usual" scenario of +4°C (SSP5–8.5) by 2080–2099 (**Fig. S1a–i**). We used a self-calibrated PDSI with Penman–Monteith potential evapotranspiration representing the current climate (1970–2000) and an intermediate and high emission scenario by 2080–2099 (SSP2–4.5 and SSP5-8.5) from Zhao and Dai (2022). The SSP2–4.5 and SSP5–8.5 scenarios were based on the average of 25 Coupled Model Intercomparison Project Phase 6 (CMIP6) models of precipitation, evapotranspiration, soil moisture, and runoff (Eyring et al., 2016), where the mean annual surface temperature is expected to increase by 2.7°C (2.1–3.5°C range) and 4.4°C (3.3–5.7°C range), respectively by 2080–2100 (IPCC, 2021). Zhao and Dai (2022) noted that there are large uncertainties in the drought projections. Therefore, our interpretation is based on the average projected drought which is typically in line with other indices of drought (Ukkola et al., 2020; Li et al., 2021; Cook et al., 2022; Zhao and Dai, 2022; Qing et al., 2023).

Anuran species richness, ecotype, and IUCN status data

We extracted the geographic range (excluding introduced range), threatened status, and ecological types of all anuran species (6,416 species) listed in the International Union for Conservation (IUCN) of Nature's Red List of Threatened Species platform (extracted on 11/01/2021; IUCN, 2022). Data-deficient Red Listed species were assigned IUCN classifications based on predictions from González-del-Pliego et al. (2019). Ecotypes were classified based on descriptions from Moen and Wiens (2017) focusing on adult behaviour and microhabitat preferences outside the breeding season given that many anurans breed in water but are not adapted to live in water all year (**Table S2**). Ecotypes were defined to provide generalised microhabitat use and for modelling the activity in different microhabitats. For example, arboreal species regularly access vertical environments like trees, rock crevices, while stream-dwelling species are restricted to permanent streams or flowing water bodies. We acknowledge that ecotype grouping does not capture the diversity of microclimate preferences. Where possible, we included secondary ecotypes in the raw data, but we analysed species based on their primary ecotype. For example, some species frequent around permanent water bodies, but occasionally have been observed climbing on trees. We would classify them primarily as 'semi-aquatic' and secondarily as 'arboreal' as they do not spend a substantial amount of time climbing. Species richness was defined as the sum of species in each grid cell (0.5°), based on the geographic range, and was calculated using the 'calcSR' function from the *rasterSp* package (https://github.com/RS-eco/rasterSp). All raster data were examined and visualised at a spatial resolution of 0.5 arc minute.

Species richness with aridity and PDSI

To examine the relationship between species richness and aridity, the number of species per grid cell was overlapped with the aridity raster layer, where each grid cell was assigned an AI category. The change in species richness between the current and projected (either +2 or +4 °C warming) AI category was calculated as the change in AI category grids occupied by anurans relative to the future projection; a lower number indicates a reduced number of species with the assigned AI category and vice versa.

With a monthly prediction of PDSI from 1950 to 2100 globally available from Zhao and Dai (2022), we classified future drought risk in three ways: 1) increase in mean drought intensity (change in PDSI or $\Delta PDSI_{[intensity]}$), increase in mean drought frequency (monthly PDSI count below -2 per year or $\Delta PDSI_{[frequency]}$), increase in mean drought duration (number of consecutive months with PDSI values below -2 or $\Delta PDSI_{[duration]}$). Change in mean $\Delta PDSI_{[intensity]}$, $\Delta PDSI_{[frequency]}$, and $\Delta PDSI_{[duration]}$ under a +2 or +4 °C warming scenario (2080–2100) was calculated relative to the 1970–2000 monthly climatology per grid cell ($\Delta PDSI = PDSI_{[future]} - PDSI_{[current]}$). Results were presented in the main text as $\Delta PDSI_{[intensity]}$, $\Delta PDSI_{[frequency]}$ and $\Delta PDSI_{[duration]}$ relative to current scenario (1970–2000). The absolute $PDSI_{[intensity]}$, $PDSI_{[frequency]}$ and $PDSI_{[duration]}$ under a +2 or +4 °C warming scenario (2080–2100) were also presented in **Fig. S2a–i**.

The simultaneous risk of increasing drought intensity, frequency, and duration within a grid cell that are occupied by anurans (species assemblages) was calculated by converting each risk category as binary. Grid cells with a $\Delta PDSI_{[intensity]}$ below -2 (indicating increased drought intensity relative to current scenario) were assigned a '1' binary. Both $\Delta PDSI_{[frequency]}$ and $\Delta PDSI_{[duration]}$ were assigned a binary of '1' if the grid cell has a value of 1 month or higher (indicating increase in frequency or duration relative to current scenario). The number of overlapping binaries were summed up per grid cell. Therefore, a risk factor of 2 indicate species assemblages in the grid cell are at increasing risk of two drought events. We estimated which species assemblages were at risk of experiencing drought events using an arbitrary risk factor scale (species richness × drought risk), where grid cells with high drought risk and high species richness have higher "assemblage-level risk" than grid cells with high drought risk and low species richness (low assemblage-level risk).

Ecotype sensitivity

Water loss and uptake data

We systematically reviewed the literature on experimental water loss and uptake studies for adult anurans following the PRISMA-EcoEvo protocol (O'Dea et al., 2021). Full detail of the systematic search, exclusion criteria, and data extraction are presented in the Supplementary Information and visualised in **Fig. S3**. Studies were included if the following hydrological metrics were reported:

water loss as the rate of evaporative water loss (EWL), resistance to water loss (total r_t or relative r_i), and change in body mass (absolute or relative), and water uptake as the rate of cutaneous water uptake (WU). Water loss measurements either by forced convection (via wind speed manipulation) or free convection (desiccant) were included in the dataset. The rate of EWL typically incorporates cutaneous and respiratory water loss as most studies do not include methods to distinguish the difference between the two routes of water loss. However, respiratory EWL is assumed to contribute little (5.5% at 25 °C) to the total EWL for amphibians (Senzano and Andrade, 2018). Additionally, the daily turnover of water for a typical amphibian from other processes such as food and water gain, metabolic water production, and urine and faecal loss is considered negligible and equivalent between species for comparative purposes (Hillman et al., 2009), thus we did not consider these aspects when comparing ecotype risks. The rate of EWL, skin resistance (r_i), and cutaneous WU were standardised to a common unit of mg h^{-1}, and s cm^{-1} for relative skin resistance using standard conversions and approximations via biophysical principles (see Supplementary Information section "Calculations and conversions").

We extracted the mean values, variance (either standard deviation or standard error), and sample size from either the study's main text, supplementary text, table, figures via metaDigitize (Pick et al., 2019), or calculated from the raw data. We also extracted the mean body mass (g), the exposed ambient temperature (°C) during the experiment, skin temperature measured (°C), coordinates of collection site (latitude and longitude in decimal degrees), flow rate (as cm s^{-1} or ml s^{-1}), duration of the experiment (min), the relative humidity (RH; %) and noted whether the animal was in a physiological water-conserving state (e.g., aestivation, cocoon-forming, or water-proof via cutaneous surface fluid or lipids). Dry air from desiccants without RH presented were assumed to be 1% RH. Missing information were obtained by contacting the study authors where possible. We noted if urine was voided prior to the EWL experiments, body mass was defined as "standard body mass" as the presence of urine will affect water loss. Additional unpublished data from 39 species of anurans were included and detailed in the 'Unpublished data' section of the Supplementary Information. Note, while we aimed for a comprehensive and representative dataset, there are geographical biases in anuran water loss and uptake studies, especially around the Amazon, central Africa, and Eurasia with high amphibian richness, but little to no water loss and uptake studies (**Fig. S4**).

Unpublished data from Brazil were collected according to the experimental procedures approved by the Ethical Committee in Animal Use (CEUA) of the Biosciences Institute (#0820), affiliated with UNESP, Rio Claro, São Paulo, Brazil. License for animal capture and transport was provided by Instituto Brasileiro do Meio Ambiente e dos Recursos Naturais Renováveis (IBAMA,

#29703-1 and 22028-1), and Secretaria do Meio Ambiente – Instituto Florestal (#26018 - 013.054/2011). Unpublished data from South Africa were collected in accordance to Western Cape Nature Permit AAA007-00073-0056, and all experimental procedures were approved by the University of Stellenbosch REC:ACU, Research Ethics Committee: Animal Care and Use (SU-ACUM13-00005).

Phylogenetic data

To account for phylogenetic relatedness in the model, we used the amphibian phylogeny of Jetz and Pyron (2018) comprising of 7,238 amphibian species. There were 5,636 species from our dataset matched the tree, and the remaining species were not available as they were described after 2016. Names were matched with the IUCN. Polytomy was removed using the function 'multi2di', and branch lengths were estimated using the 'compute.brlen' function from the *ape* package (Paradis and Schliep, 2018). The generated tree was converted to a phylogenetic relatedness correlation matrix for subsequent analysis.

Water loss and uptake analyses

All models used a No-U-Turn Sampler extension of Hamiltonian Monte Carlo (Hoffman and Gelman, 2014) Bayesian procedure implemented in the *R* package *brms* (Bürkner, 2017) to derive posterior distributions and associated credible intervals (CIs) for the fitted parameters. For all models, we constructed four chains with 5,000 steps per chain, including 2,500-step warm-up periods, hence a total of 10,000 steps were retained to estimate posterior distributions [i.e., (5,000 − 2,500) × 4 = 10,000]. Adapt delta was set at 0.99 to decrease the number of divergent transitions, and the maximum tree depth was set to 15 when the depth of tree evaluated in each iteration was exceeded. Fixed effects were assigned weakly informative priors following a Gaussian distribution ($\ln\beta_0$ mean = 0, SD = 3) to speed up model convergence, and Student's t prior with three degrees of freedom was used for group-level, hierarchical effects. The degree of convergence of the model was deemed as achieved when the Gelman–Rubin statistics, $\hat{R}$ (Gelman and Rubin, 1992), was 1.

Differences in resistance to water loss (r_i) and WU between ecotypes were examined with the 'brms' function from the *brms* package. We analysed r_i because it represents the most physiologically relevant metric of water loss (Feder and Burggren, 1992; Riddell et al., 2017). For the r_i water loss model, we included the natural logarithm transformed body mass (lnMass), VPD (lnVPD), and air flow rate (lnFlow) as additive fixed effects. Study ID, lnMass nested in species, and the phylogenetic correlation matrix were included as group-level effects to account for variance between studies, repeated measures within species, and evolutionary history (Pottier et al., 2024a). For the WU model, the fixed effects were lnMass, treatment temperature, and initial hydration level. Relative humidity was never reported during the WU experiments, thus VPD was replaced with

exposure temperature. Group-level effects were the same as for the water loss model. Only ecotypes with five or more recordings were analysed (Nakagawa et al., 2017). The R^2_{marginal} and $R^2_{\text{conditional}}$ were calculated from the water loss and WU models using the 'r2_bayes' function from the *performance* package (Lüdecke et al., 2021), and posterior predictive checks were presented in Supplementary **Fig. S5**. All statistical outcomes are presented as mean posterior estimates ± 95% credible intervals (95% CI). The model results were also visualised in **Fig. S6–7**.

Water loss vulnerability

We estimated the impact of SSP2–4.5 (+2 °C) and SSP5–8.5 (+4 °C) scenarios on EWL globally for a typical 8.7 g frog (geometric mean body mass of the study) using the 'ectotherm' function from the *NicheMapR* package (Kearney and Porter, 2020) and compared the estimated EWL to the spatial distribution of species richness. We extracted high resolution (~4km^2) global dataset on the mean VPD (kPA/month) and mean wind speed (m s^{-1}/month) from Abatzoglou et al. (2018) under the current climate (1970–2000) and under a +2 and +4°C scenario to estimate EWL under the current and future scenario. Wind speed at ground level (1 cm) was corrected based on the reference height of 10 m and assuming a level surface roughness of 0.15 m in an open landscape (https://mrke.github.io/NicheMapR/inst/doc/microclimate-model-theory-equations).

Effect of environmental warming and drying on behavioural activity

To demonstrate the role of water-conserving strategies on the potential hours for activity, we simulated a hypothetical frog in Karawatha, Queensland, Australia. Karawatha has a record of daily rainfall from 1994–current and this area has experienced drought recently (2017–2019). The aim is to explore the interactions between different climate processes on frog activity rather than reflect realistic changes in the ecosystem. We also note that these simulations can be applied to any terrestrial location in the world with species-specific thermal and hydrological variables.

We used *NicheMapR* to construct a biophysical model of the water, and energy balance of a typical adult frog (8.7 g) from Kearney and Porter (2020) and Kearney and Enriquez-Urzelai (2022) to test the role of behavioural and physiological regulation on potential activity under different thermal and hydric conditions. The default frog model was based on the leopard frog *Lithobates pipiens* and was applied for all ecotypes because r_i and WU rate did not differ between ecotypes (**Table S3–4**). The model was based on the 'thermodynamic niche' modelling scheme, considering thermodynamic effects on the biophysical landscape (**Fig. S8a**). Three hypothetical frog models with differing water saving strategies were simulated to estimate the influence of behaviour and physiological modification on activity (summarised in **Table S5**): 1) a shade model where the frog can thermo-hydroregulate with shade available (0–90% shade), but is not able to burrow or climb up trees to regulate temperature and hydration (representative of a typical ground-dwelling frog), 2)

an arboreal model with water-proof skin (high skin resistance) and the ability to climb trees up to 150 cm high to regulate their body temperature and hydration (representative of arboreal frog), 3) burrowing model where the frog is able to burrow underground to a maximum of 200 cm to regulate body temperature and hydration (representative of fossorial species). Semi-aquatic and stream-dwelling ecotypes were not simulated as they are typically found around permanent water bodies, which allows them to quickly rehydrate; our models focused on activity change under terrestrial conditions.

We simulated the potential hours (in a 24 hour day) active in a year (t_{act}) which represents the suitable thermal and hydric conditions for the animal to move beyond their retreat to either catch prey or find mates (Kearney and Porter, 2020). While frogs can survive losing up to 50% of their body weight before death (Hillman et al., 2009), locomotor performance declines rapidly around 10–30% loss of water (Beuchat et al., 1984; Titon Jr et al., 2010; Anderson and Andrade, 2017; Greenberg and Palen, 2021), and toads have been observed to seek shade after losing ~14% of their water mass (Bartelt, 2000). Therefore, we used a threshold of 80% of hydrated body mass to stop activity, as locomotion is highly impaired below these conditions.

For each hypothetical frog model, we simulated t_{act} under four climate conditions, 1) current normal scenario (typical air temperature and rainfall), 2) a current drought scenario (typical air temperature and low rainfall), 3) a warming normal scenario (+4°C only), and 4) a warming drought scenario (+4°C and low rainfall). Vapour pressure was computed from the environmental temperature and humidity values which directly affects EWL in the model (driven by the vapour density gradient between the skin surface and the air), while the simulated soil water potential influences WU rate (Kearney and Enriquez-Urzelai, 2022). The full detail of model specifications and climate model verification are provided in the Supplementary Information "*NicheMapR*" section and **Fig. S9**.

RESULTS

Species richness, aridity, and drought risk

Amphibian species richness is inversely correlated with the aridity, where the higher the AI, the fewer amphibian species per grid cell (**Fig. 1a-c**). On average, most species classified as stream-dwellers inhabit wetter regions (mean AI of 1.46 ± 0.62 s.d), while most fossorial species live in drier regions (mean AI of 0.80 ± 0.61 s.d; **Fig. 1d**). Under an intermediate warming scenario of +2°C, around 6.6% of areas occupied by anurans will increase to arid-like conditions. Humid regions will reduce by 1.4%, dry sub-humid regions will increase by 2.5%, semi-arid regions will increase by 1.4%, arid regions will increase by 5% and hyper-arid regions will decrease by 2.3% (**Fig. 1e** and **1f**). Under a high warming scenario of +4°C, around 33.5% of areas occupied by all

anurans will increase to arid-like conditions. Humid regions will reduce by 5.8%, dry sub-humid regions will increase by 9%, semi-arid regions will increase by 8.4%, arid regions will increase by 13.2% and hyper-arid regions will increase by 3% (**Fig. 1e** and **1g**).

By 2080–2100, 15.4 % of regions occupied by anurans are expected to face a combination of increased drought in relation to the three metrics we considered: intensity, frequency, and duration. This is especially so in large areas of South America, northern America, and most of eastern Europe under an intermediate emission scenario (SPP2–4.5; **Fig. 2a**). Under a high emission scenario (SPP5–8.5), 36.1 % of regions occupied by anurans, mainly the Americas, southern Africa, Europe, and southern Australia, will be at risk of increased exposure to drought according to all three metrics (**Fig. 2b**). Anuran species-assemblages in the Amazon region had the highest risk from the combination of high species richness and is predicted to be exposed to increases in all three metrics under both intermediate and high emission scenario (**Fig. 2c–d**).

We estimate around 21% of regions that anurans occupy will be at risk of increasing drought intensity under an intermediate scenario (**Extended Data Fig. 1a–b**). Under a high emission scenario, 38% of the area anurans occupy will be at risk of increasing drought intensity (**Extended Data Fig. 1c–d**). Anurans in central America, southern America, western and central Europe, southern Africa, and southern Australia are expected to be subjected to increased average drought frequency by 1–4 months per year under an intermediate emission scenario (41.1% of areas occupied by anurans; **Extended Data Fig. 2a–b**), while the mean frequency of over 4 months per year are considered rare (0.9%). 15.3% of regions occupied by anurans are expected to reduce in the frequency of drought. Under a high emission scenario, anurans in central America, the Amazon region, Chile, northern United States, and the Mediterranean regions are predicted to experience increases in drought frequency by over 4 months per year (16.3% of areas occupied by amphibians more than 4 months per year; **Extended Data Fig. 2c–d**). 27.4% of regions occupied by anurans are not expected to change and 11% are expected to reduce in drought frequency.

The duration of drought will increase in most of the America's, Europe, southern and central Africa, and southern Australia by 1–4 consecutive months under an intermediate emission scenario (28.6% of areas occupied by anurans; **Extended Data Fig. 3a–b**). The mean durations of over 4 months occurred over a limited area (3.1%). Some areas are expected experience increases in drought duration by 10 months in the northern United States, Honduras, the Amazon region, Guyana, Chile, Spain, and Türkiye (1.6% of areas occupied by anurans; **Extended Data Fig. 3c–d**).

Water loss and uptake

Resistance to water loss (r_i) did not differ between ecotypes but varied by water-conserving strategies (**Table S3**; **Fig. S6**). Frogs with water-proof skin (morphological), with a cocoon layer during aestivation (physiological), and inside artificial hollow structures (behavioural) had higher r_i than frogs with no specialised water conserving strategies, with the highest r_i from frogs that are in aestivation (**Fig. S6b**). Body size, and flow rate influenced r_i, which explained 64% [60–68] of the variation in r_i (**Table S3**). r_i increased with body mass with a scaling exponent of 0.10 [0.04–0.17], and higher wind speed decreased r_i (-0.22 [-0.34–-0.10]). There was a moderate phylogenetic signal for water loss (λ = 0.38 [0.04–0.65]). EWL was high for a 8.7 g frog in regions with high annual VPD (indicator of dryness) such as hot, arid regions (**Fig. 3a**). Anuran species richness is negatively related to the potential EWL where areas with climates that allow low EWL have a higher number of anuran species (**Fig. 3b**). Under an intermediate and high-emission scenario, EWL increased the most in arid regions (**Fig. 3c-d**), where EWL nearly doubles in the Sahara, Arabian, Taklamakan, and Australian deserts under a high-emission scenario (**Fig. 3d**).

Water uptake did not differ between ecotypes or treatment temperature (**Table S4**). However, water uptake was influenced by body size and initial hydration, both moderators explained 69% [62–75] of the variation in water uptake (**Extended Data Fig. S5**). WU increased with body mass with a scaling exponent of 0.80 [0.70–0.91], and more dehydrated frogs had higher water uptake rates (-0.5 [-0.7– -0.04). There was a strong phylogenetic signal for water uptake (λ = 0.78 [0.38–0.94]).

Effect of environmental warming and drying on behavioural activity

Biophysical simulations of the current climate scenario (no warming, no drought) in Karawatha, Queensland, showed a hypothetical ground-dwelling frog could be active 3,971 hours out of 8,760 total hours of the year (45%) (**Fig. 4a**). The corresponding values for a water-proof arboreal frog was 4,767 h (54%), and 4,286 h (49%) for a burrowing frog (**Fig. 4c and e**).

Under a warming climate scenario alone (+4 °C, no drought), the ground-dwelling frog increased in potential activity by 346 h (8.8%), the waterproof arboreal frog by 197 h (3.6%), and the burrowing frog by 428 h (10%) relative to the current climate scenario. The increase in activity was driven by warmer winters (June to August) allowing for more activity during the coldest quarter (**Fig. 4b, d, g**, **Table S6**). When restricted to the warmest quarter of the year (December to February), where climate warming is predicted to have the greatest impact, warming decreased activity by 8.5% for a ground-dwelling frog, 8.8% for a waterproof frog, and 4.6% for a burrowing frog (**Table S6**).

Under a drought climate scenario (no warming, drought) matching the 2018–2019 historical drought, the ground-dwelling frog decreased potential activity by 174 h (4.5%), the waterproof arboreal frog by 192 h (4.5%), and the burrowing frog by 97 h (2.2%) across the year. The effects of drought were highest in the warmest quarter with an average reduction in potential activity for all ecotypes by 8.3% relative to the current scenario (**Table S6**). When simulating both warming and drought climate scenarios together, the ground-dwelling frog decreases its potential activity by 188 h (17.7% reduction), the waterproof arboreal frog by 224 h (19%), and the burrowing frog by 125 h (10%) relative to the current scenario in the warmest quarter. For all ecotypes, a reduction in rainfall has a greater effect on yearly activity than an increase in temperature alone (**Table S6**).

DISCUSSION

Amphibians are the most threatened class of vertebrates, and the number of species directly impacted by climate change has increased by 39% over the last decade (Luedtke et al., 2023). We find the exposure risk of anurans to increasing environmental dryness is global with most regions where anurans occupy increasing in the average aridity and in the intensity, frequency, and duration of extreme drought events. The Amazon rainforest in South America is of particular concern because high species diversity overlaps with high risk to increasing drought. Our results demonstrate how combining the effects of temperature and environmental dryness is more impactful for amphibians' biology, thus providing a more comprehensive understanding of the vulnerability of ectotherms to climate change.

Stream-dwelling or semi-aquatic ecotypes are expected to have a greater risk of water loss than arboreal or fossorial ecotypes due to differences in adaptation to differing water exposure in their environment. However, similarities in skin resistance and WU across all ecotypes in our study suggest habitat preference does not drive variation in water loss and WU as suggested in previous studies (Thorson, 1955; Katz and Graham, 1980; Withers et al., 1984; Wygoda, 1984). Instead, a species' risk of water loss may be more tightly related to physiological and behavioural traits. For example, some arboreal species have lower rates of EWL due to their high skin resistance than other ecotypes. The high skin resistance may be attributed to either secretions (mucus, lipids, proteins) or iridophores (Lillywhite, 2006) that allow some "waterproof" species to have r_i values as high as squamates, turtles, and crocodylians (Hillman et al., 2009). Concerning the vulnerability to climate change, most anuran species (apart from waterproof and cocoon-forming frogs) lack physiological ways to reduce EWL. Such species must therefore rely on behavioural hydroregulation such as microhabitat shelter to reduce dehydration risk (Schwarzkopf and Alford, 1996; de Andrade and Abe, 1997; Seebacher and Alford, 2002), otherwise it is expected that EWL may double in arid regions in open habitats under a high-emission scenario (**Fig. 3d**).

The spatial extent of increasing drought events tends to overlap with extreme thermal events described by Murali et al. (2023). Heatwaves are typically most frequent and intense in arid regions (Murali et al., 2023), but these areas tend to have few if any anuran species. Of serious concern are anurans in tropical regions such as the Amazon borders and southeast Asia that may experience extreme drought and extreme warming (Malhi et al., 2008; Phillips et al., 2009). The combined effects drought and warming could act synergistically on physiological functions in ways that further reduce potential activity and survival. For example, the thermal tolerance and preferred body temperature tend to decrease as frogs are dehydrated or subjected to dry conditions (Mitchell and Bergmann, 2016; Anderson and Andrade, 2017; Guevara-Molina et al., 2020). Likewise, amphibians under heat stress will attempt to keep cool via evaporative cooling. When exposed to 40–50°C air temperatures, anurans can maintain a skin surface temperature around 35°C (**Fig. S11**). However, this comes at a cost of increased EWL. The negative effects of high temperature on frog locomotor performance is exacerbated by dehydration in anurans (Preest and Pough, 1989; Walvoord, 2003). Because extreme atmospheric evaporative demand under rising temperatures and less predictable rainfall will impact the biology and phenology of terrestrial organism that depend on water, the interactions of water and temperature must be considered for accurate forecasting of physiological vulnerability to climate change (Rozen-Rechels et al., 2019; Lertzman-Lepofsky et al., 2020).

Dehydration impacts on behavioural activity are ecologically important because physiological-based restrictions on activity can limit the ability of organisms to disperse (Wu and Seebacher, 2022), and shorten the time window for breeding (Wassens et al., 2013). The reduction in activity when dehydrated is likely due to decline in ability to synthesise ATP by aerobic means and increase in glycolysis during locomotion under water stress (Gatten Jr, 1987). However, drought may not only reduce foraging and mating seeking opportunities, but also the environmental resource available to fuel locomotion. Environmental aridity is highly correlated with primary productivity and, therefore, food availability (Janzen and Schoener, 1968; Qiu et al., 2023). Thus, environmental drying restricts both the quantity of available food as well as the capacity to find it (Lertzman-Lepofsky et al., 2020). Due to the paucity of amphibian studies directly linking environmental drying and activity in the field (Tracy et al., 2013), our understanding of amphibian sensitivity would benefit from field research focused on species-specific changes in activity in regions to be most at risk to drying.

Physiological plasticity can increase an organism's resistance to climate change (Seebacher et al., 2015). Whether amphibians can adapt to increasing environmental dryness will depend on their acclimation capacity. Previous research have indicated amphibians acclimation to drier

conditions by increased skin resistance (Wygoda, 1988), and regenerated capillary beds in the skin (Riddell et al., 2019) which help increase WU capacity. Whether these changes permit longer activity under drier conditions requires further investigation, especially for small, narrowly distributed species, as observed in insects (Hoffmann et al., 2003; Chown et al., 2011). Field observations have shown frog community assemblages are larger in average size in warmer, drier regions (Guo et al., 2019; Castro et al., 2021; Sheridan et al., 2022). Larger frogs have lower EWL proportionally to smaller frogs, and have higher water storing capacity in the bladder (Hillman et al., 2009). Therefore, we may observe phenotypic change in amphibian community composition, where larger species may be able to cope better with increased environmental drying relative to smaller species. Consideration of plasticity is important for evaluating species risk to climate change because plasticity can often, but not always, buffer the effects of environmental stressors (Wu and Seebacher, 2021), and not accounting for plasticity and evolutionary potential can overestimate the impacts of environmental change on predicting species distributions (Gerick et al., 2014; Kellermann et al., 2020).

To understand and manage the effects of climate change on biodiversity we must integrate knowledge on the biologically relevant processes for different types of organism in different habitats. Thermal constraints on activity are often a focus for studies of ectotherms but integrating thermal and hydric constraints gives a deeper understanding of anurans and other wet-skinned terrestrial organisms risk to climate change than temperature alone.

REFERENCES

Abatzoglou, J. T., Dobrowski, S. Z., Parks, S. A. and Hegewisch, K. C. (2018). TerraClimate, a high-resolution global dataset of monthly climate and climatic water balance from 1958–2015. *Scientific data* **5**, 170191.

Albright, T. P., Mutiibwa, D., Gerson, A. R., Smith, E. K., Talbot, W. A., O'Neill, J. J., McKechnie, A. E. and Wolf, B. O. (2017). Mapping evaporative water loss in desert passerines reveals an expanding threat of lethal dehydration. *Proc. Natl. Acad. Sci.* **114**, 2283-2288.

Amey, A. P. and Grigg, G. C. (1995). Lipid-reduced evaporative water loss in two arboreal hylid frogs. *Comp. Biochem. Physiol. Part A Physiol.* **111**, 283-291.

Anderson, R. C. and Andrade, D. V. (2017). Trading heat and hops for water: dehydration effects on locomotor performance, thermal limits, and thermoregulatory behavior of a terrestrial toad. *Ecol. Evol.* **7**, 9066-9075.

Bartelt, P. E. (2000). A biophysical analysis of habitat selection in western toads (*Bufo boreas*) in southeastern Idaho. *PhD*. Department of Biology, Idaho State University.

Beuchat, C. A., Pough, F. H. and Stewart, M. M. (1984). Response to simultaneous dehydration and thermal stress in three species of Puerto Rican frogs. *J. Comp. Physiol. B* **154**, 579-585.

Budyko, M. I. (1961). The heat balance of the earth's surface. *Soviet Geography* **2**, 3-13.

Bürkner, P.-C. (2017). brms: an R package for Bayesian multilevel models using Stan. *J. Stat. Softw.* **80**, 1-28.

Campbell Grant, E. H., Miller, D. A. and Muths, E. (2020). A synthesis of evidence of drivers of amphibian declines. *Herpetologica* **76**, 101-107.

Carvalho, J. E., Navas, C. A. and Pereira, I. C. (2010). Energy and water in aestivating amphibians. In *Aestivation: molecular and physiological aspects*, eds. C. A. Navas and J. E. Carvalho), pp. 141-169. Heidelberg, Germany: Springer.

Castro, K. M., Amado, T. F., Olalla-Tárraga, M. Á., Gouveia, S. F., Navas, C. A. and Martinez, P. A. (2021). Water constraints drive allometric patterns in the body shape of tree frogs. *Sci. Rep.* **11**, 1218.

Cherlet, M., Hutchinson, C., Reynolds, J., Hill, J., Sommer, S. and von Maltitz, G. (2018). World atlas of desertification. Luxembourg: Publication Office of the European Union.

Chown, S. L., Sørensen, J. G. and Terblanche, J. S. (2011). Water loss in insects: an environmental change perspective. *J. Insect Physiol.* **57**, 1070-1084.

Cook, B. I., Smerdon, J. E., Cook, E. R., Williams, A. P., Anchukaitis, K. J., Mankin, J. S., Allen, K., Andreu-Hayles, L., Ault, T. R. and Belmecheri, S. (2022). Megadroughts in the Common Era and the Anthropocene. *Nature Reviews Earth & Environment* **3**, 741-757.

Dai, A., Trenberth, K. E. and Qian, T. (2004). A global dataset of Palmer Drought Severity Index for 1870–2002: relationship with soil moisture and effects of surface warming. *J. Hydrometeorol.* **5**, 1117-1130.

de Andrade, D. V. and Abe, A. S. (1997). Evaporative water loss and oxygen uptake in two casque-headed tree frogs, *Aparasphenodon brunoi* and *Corythomantis greeningi* (Anura, Hylidae). *Comp. Biochem. Physiol. Part A Physiol.* **118**, 685-689.

Eamus, D., Boulain, N., Cleverly, J. and Breshears, D. D. (2013). Global change-type drought-induced tree mortality: vapor pressure deficit is more important than temperature per se in causing decline in tree health. *Ecol. Evol.* **3**, 2711-2729.

Eyring, V., Bony, S., Meehl, G. A., Senior, C. A., Stevens, B., Stouffer, R. J. and Taylor, K. E. (2016). Overview of the Coupled Model Intercomparison Project Phase 6 (CMIP6) experimental design and organization. *Geoscientific Model Development* **9**, 1937-1958.

Feder, M. E. and Burggren, W. W. (1992). Environmental physiology of the amphibians. Chicago, USA: University of Chicago Press.

Ficetola, G. F. and Maiorano, L. (2016). Contrasting effects of temperature and precipitation change on amphibian phenology, abundance and performance. *Oecologia* **181**, 683-693.

Galindo, C., Cruz, E. and Bernal, M. (2018). Evaluation of the combined temperature and relative humidity preferences of the Colombian terrestrial salamander *Bolitoglossa ramosi* (Amphibia: Plethodontidae). *Can. J. Zool.* **96**, 1230-1235.

Gatten Jr, R. E. (1987). Activity metabolism of anuran amphibians: tolerance to dehydration. *Physiol. Zool.* **60**, 576-585.

Gelman, A. and Rubin, D. B. (1992). Inference from iterative simulation using multiple sequences. *Stat. Sci.* **7**, 457-472.

Gerick, A. A., Munshaw, R. G., Palen, W. J., Combes, S. A. and O'Regan, S. M. (2014). Thermal physiology and species distribution models reveal climate vulnerability of temperate amphibians. *J. Biogeogr.* **41**, 713-723.

González-del-Pliego, P., Freckleton, R. P., Edwards, D. P., Koo, M. S., Scheffers, B. R., Pyron, R. A. and Jetz, W. (2019). Phylogenetic and trait-based prediction of extinction risk for data-deficient amphibians. *Curr. Biol.* **29**, 1557-1563. e1553.

Greenberg, D. A. and Palen, W. J. (2021). Hydrothermal physiology and climate vulnerability in amphibians. *Proc. R. Soc. B.* **288**, 20202273.

Grossiord, C., Buckley, T. N., Cernusak, L. A., Novick, K. A., Poulter, B., Siegwolf, R. T., Sperry, J. S. and McDowell, N. G. (2020). Plant responses to rising vapor pressure deficit. *New Phytol.* **226**, 1550-1566.

Guevara-Molina, E. C., Gomes, F. R. and Camacho, A. (2020). Effects of dehydration on thermoregulatory behavior and thermal tolerance limits of *Rana catesbeiana* (Shaw, 1802). *J. Therm. Biol.* **93**, 102721.

Gunderson, A. R. and Stillman, J. H. (2015). Plasticity in thermal tolerance has limited potential to buffer ectotherms from global warming. *Proc. R. Soc. B. Biol. Sci.* **282**, 20150401.

Guo, C., Gao, S., Krzton, A. and Zhang, L. (2019). Geographic body size variation of a tropical anuran: effects of water deficit and precipitation seasonality on Asian common toad from southern Asia. *BMC Evol. Biol.* **19**, 1-11.

Hillman, S. S., Withers, P. C., Drewes, R. C. and Hillyard, S. D. (2009). Ecological and environmental physiology of amphibians. New York, USA: Oxford University Press

Hoffman, M. D. and Gelman, A. (2014). The No-U-Turn sampler: adaptively setting path lengths in Hamiltonian Monte Carlo. *J. Mach. Learn. Res.* **15**, 1593-1623.

Hoffmann, A., Hallas, R., Dean, J. and Schiffer, M. (2003). Low potential for climatic stress adaptation in a rainforest Drosophila species. *Science* **301**, 100-102.

Iknayan, K. J. and Beissinger, S. R. (2018). Collapse of a desert bird community over the past century driven by climate change. *Proc. Natl. Acad. Sci.* **115**, 8597-8602.

IPCC. (2021). Climate Change 2021: The Physical Science Basis, Contribution of Working Group I to the Sixth Assessment Report of the Intergovernmental Panel on Climate Change, eds V. Masson-Delmotte P. Zhai A. Pirani S. L. Connors C. Péan S. Berger N. Caud Y. Chen L. Goldfarb M. I. Gomis et al.). Cambridge, UK.

IUCN. (2022). The IUCN Red List of threatened species. Version 2022-2. <https://www.iucnredlist.org/>

Janzen, D. H. and Schoener, T. W. (1968). Differences in insect abundance and diversity between wetter and drier sites during a tropical dry season. *Ecology* **49**, 96-110.

Jetz, W. and Pyron, R. A. (2018). The interplay of past diversification and evolutionary isolation with present imperilment across the amphibian tree of life. *Nat. Eco. Evol.* **2**, 850-858.

Katz, U. and Graham, R. (1980). Water relations in the toad (*Bufo viridis*) and a comparison with the frog (*Rana ridibunda*). *Comp. Biochem. Physiol. Part A Physiol.* **67**, 245-251.

Kearney, M. R. and Porter, W. P. (2020). NicheMapR–an R package for biophysical modelling: the ectotherm and Dynamic Energy Budget models. *Ecography* **43**, 85-96.

Kearney, M. R. and Enriquez-Urzelai, U. (2022). A general framework for jointly modelling thermal and hydric constraints on developing eggs. *Method. Ecol. Evol.*

Kearney, M. R., Porter, W. P. and Murphy, S. A. (2016). An estimate of the water budget for the endangered night parrot of Australia under recent and future climates. *Climate Change Responses* **3**, 1-17.

Kearney, M. R., Munns, S. L., Moore, D., Malishev, M. and Bull, C. M. (2018). Field tests of a general ectotherm niche model show how water can limit lizard activity and distribution. *Ecol. Monogr.* **88**, 672-693.

Kellermann, V., McEvey, S. F., Sgrò, C. M. and Hoffmann, A. A. (2020). Phenotypic plasticity for desiccation resistance, climate change, and future species distributions: will plasticity have much impact? *Am. Nat.* **196**, 306-315.

Kohli, A. K., Lindauer, A. L., Brannelly, L. A., Ohmer, M. E., Richards-Zawacki, C., Rollins-Smith, L. and Voyles, J. (2019). Disease and the drying pond: examining possible links among drought, immune function, and disease development in amphibians. *Physiol. Biochem. Zool.* **92**, 339-348.

Kupferberg, S. J., Moidu, H., Adams, A. J., Catenazzi, A., Grefsrud, M., Bobzien, S., Leidy, R. and Carlson, S. M. (2022). Seasonal drought and its effects on frog population dynamics and amphibian disease in intermittent streams. *Ecohydrology* **15**, e2395.

Lertzman-Lepofsky, G. F., Kissel, A. M., Sinervo, B. and Palen, W. J. (2020). Water loss and temperature interact to compound amphibian vulnerability to climate change. *Glob. Chang. Biol.* **26**, 4868-4879.

Li, H., Li, Z., Chen, Y., Xiang, Y., Liu, Y., Kayumba, P. M. and Li, Z. (2021). Drylands face potential threat of robust drought in the CMIP6 SSPs scenarios. *Environ. Res. Lett.* **16**, 114004.

Li, Y., Cohen, J. M. and Rohr, J. R. (2013). Review and synthesis of the effects of climate change on amphibians. *Integr. Zool.* **8**, 145-161.

Lillywhite, H. B. (2006). Water relations of tetrapod integument. *J. Exp. Biol.* **209**, 202-226.

Lowe, W. H., Martin, T. E., Skelly, D. K. and Woods, H. A. (2021). Metamorphosis in an era of increasing climate variability. *Trends Ecol. Evol.* **36**, 360-375.

Lüdecke, D., Ben-Shachar, M. S., Patil, I., Waggoner, P. and Makowski, D. (2021). performance: an R package for assessment, comparison and testing of statistical models. *Journal of Open Source Software* **6**, 3139.

Luedtke, J. A., Chanson, J., Neam, K., Hobin, L., Maciel, A. O., Catenazzi, A., Borzée, A., Hamidy, A., Aowphol, A. and Jean, A. (2023). Ongoing declines for the world's amphibians in the face of emerging threats. *Nature*, 1-7.

Malhi, Y., Roberts, J. T., Betts, R. A., Killeen, T. J., Li, W. and Nobre, C. A. (2008). Climate change, deforestation, and the fate of the Amazon. *Science* **319**, 169-172.

Mitchell, A. and Bergmann, P. J. (2016). Thermal and moisture habitat preferences do not maximize jumping performance in frogs. *Funct. Ecol.* **30**, 733-742.

Moen, D. S. and Wiens, J. J. (2017). Microhabitat and climatic niche change explain patterns of diversification among frog families. *Am. Nat.* **190**, 29-44.

Murali, G., Iwamura, T., Meiri, S. and Roll, U. (2023). Future temperature extremes threaten land vertebrates. *Nature*.

Nakagawa, S., Noble, D. W., Senior, A. M. and Lagisz, M. (2017). Meta-evaluation of meta-analysis: ten appraisal questions for biologists. *BMC biology* **15**, 1-14.

Navas, C. A., Antoniazzi, M. M., Carvalho, J. E., Suzuki, H. and Jared, C. (2007). Physiological basis for diurnal activity in dispersing juvenile *Bufo granulosus* in the Caatinga, a Brazilian semi-arid environment. *Comp. Biochem. Physiol. Part A Mol. Integr. Physiol.* **147**, 647-657.

O'Dea, R. E., Lagisz, M., Jennions, M. D., Koricheva, J., Noble, D. W., Parker, T. H., Gurevitch, J., Page, M. J., Stewart, G. and Moher, D. (2021). Preferred reporting items for systematic reviews and meta-analyses in ecology and evolutionary biology: a PRISMA extension. *Biol. Rev.* **96**, 1695-1722.

Palmer, W. C. (1965). Meteorological drought. Washington DC, USA: US Department of Commerce, Weather Bureau.

Paradis, E. and Schliep, K. (2018). ape 5.0: an environment for modern phylogenetics and evolutionary analyses in R. *Bioinformatics* **35**, 526-528.

Park Williams, A., Allen, C. D., Macalady, A. K., Griffin, D., Woodhouse, C. A., Meko, D. M., Swetnam, T. W., Rauscher, S. A., Seager, R. and Grissino-Mayer, H. D. (2013). Temperature as a potent driver of regional forest drought stress and tree mortality. *Nat. Clim. Change* **3**, 292-297.

Phillips, O. L., Aragão, L. E., Lewis, S. L., Fisher, J. B., Lloyd, J., López-González, G., Malhi, Y., Monteagudo, A., Peacock, J. and Quesada, C. A. (2009). Drought sensitivity of the Amazon rainforest. *Science* **323**, 1344-1347.

Pick, J. L., Nakagawa, S. and Noble, D. W. (2019). Reproducible, flexible and high-throughput data extraction from primary literature: the metaDigitise R package. *Method. Ecol. Evol.* **10**, 426-431.

Pokhrel, Y., Felfelani, F., Satoh, Y., Boulange, J., Burek, P., Gädeke, A., Gerten, D., Gosling, S. N., Grillakis, M. and Gudmundsson, L. (2021). Global terrestrial water storage and drought severity under climate change. *Nat. Clim. Change* **11**, 226-233.

Pottier, P., Noble, D. W., Seebacher, F., Wu, N. C., Lagisz, M., Schwanz, L., Drobniak, S. M. and Nakagawa, S. (2024a). New horizons for comparative studies and meta-analyses. *Trends Ecol. Evol.*

Pottier, P., Kearney, M. R., Wu, N. C., Gunderson, A. R., Reij, J. E., Reivera-Villanueva, N., Pollo, P., Burke, S., Drobniak, S. M. and Nakagawa, S. (2024b). Vulnerability of amphibians to global warming. *EcoEvoRxiv*.

Pough, F. H., Taigen, T. L., Stewart, M. M. and Brussard, P. F. (1983). Behavioral modification of evaporative water loss by a Puerto Rican frog. *Ecology* **64**, 244-252.

Preest, M. and Pough, F. H. (1989). Interaction of temperature and hydration on locomotion of toads. *Funct. Ecol.* **3**, 693-699.

Qing, Y., Wang, S., Yang, Z.-L., Gentine, P., Zhang, B. and Alexander, J. (2023). Accelerated soil drying linked to increasing evaporative demand in wet regions. *npj Climate and Atmospheric Science* **6**, 205.

Qiu, R., Han, G., Li, S., Tian, F., Ma, X. and Gong, W. (2023). Soil moisture dominates the variation of gross primary productivity during hot drought in drylands. *Sci. Total Environ.* **899**, 165686.

Riddell, E. A., Apanovitch, E. K., Odom, J. P. and Sears, M. W. (2017). Physical calculations of resistance to water loss improve predictions of species range models. *Ecol. Monogr.* **87**, 21-33.

Riddell, E. A., Roback, E. Y., Wells, C. E., Zamudio, K. R. and Sears, M. W. (2019). Thermal cues drive plasticity of desiccation resistance in montane salamanders with implications for climate change. *Nat. Commun.* **10**, 4091.

Rozen-Rechels, D., Dupoué, A., Lourdais, O., Chamaillé-Jammes, S., Meylan, S., Clobert, J. and Le Galliard, J. F. (2019). When water interacts with temperature: ecological and evolutionary implications of thermo-hydroregulation in terrestrial ectotherms. *Ecol. Evol.* **9**, 10029-10043.

Schwarzkopf, L. and Alford, R. (1996). Desiccation and shelter-site use in a tropical amphibian: comparing toads with physical models. *Funct. Ecol.*, 193-200.

Seebacher, F. and Alford, R. A. (2002). Shelter microhabitats determine body temperature and dehydration rates of a terrestrial amphibian (*Bufo marinus*). *J. Herpetol.* **36**, 69-75.

Seebacher, F., White, C. R. and Franklin, C. E. (2015). Physiological plasticity increases resilience of ectothermic animals to climate change. *Nat. Clim. Change* **5**, 61-66.

Senzano, L. M. and Andrade, D. V. (2018). Temperature and dehydration effects on metabolism, water uptake and the partitioning between respiratory and cutaneous evaporative water loss in a terrestrial toad. *J. Exp. Biol.* **221**, jeb188482.

Sheridan, J. A., Mendenhall, C. D. and Yambun, P. (2022). Frog body size responses to precipitation shift from resource-driven to desiccation-resistant as temperatures warm. *Ecol. Evol.* **12**, e9589.

Shoemaker, V. H. and McClanahan, L. L. (1980). Nitrogen excretion and water balance in amphibians of Borneo. *Copeia* **3**, 446-451.

Slette, I. J., Post, A. K., Awad, M., Even, T., Punzalan, A., Williams, S., Smith, M. D. and Knapp, A. K. (2019). How ecologists define drought, and why we should do better. *Glob. Chang. Biol.* **25**, 3193-3200.

Snyder, G. K. and Weathers, W. W. (1975). Temperature adaptations in amphibians. *Am. Nat.* **109**, 93-101.

Sodhi, N. S., Bickford, D., Diesmos, A. C., Lee, T. M., Koh, L. P., Brook, B. W., Sekercioglu, C. H. and Bradshaw, C. J. (2008). Measuring the meltdown: drivers of global amphibian extinction and decline. *PloS one* **3**, e1636.

Spinoni, J., Barbosa, P., Bucchignani, E., Cassano, J., Cavazos, T., Christensen, J. H., Christensen, O. B., Coppola, E., Evans, J. and Geyer, B. (2020). Future global meteorological drought hot spots: A study based on CORDEX data. *Journal of Climate* **33**, 3635-3661.

Stinner, J. N. and Shoemaker, V. H. (1987). Cutaneous gas exchange and low evaporative water loss in the frogs *Phyllomedusa sauvagei* and *Chiromantis xerampelina*. *J. Comp. Physiol. B* **157**, 423-427.

Thorson, T. B. (1955). The relationship of water economy to terrestrialism in amphibians. *Ecology* **36**, 100-116.

Titon Jr, B., Navas, C. A., Jim, J. and Gomes, F. R. (2010). Water balance and locomotor performance in three species of neotropical toads that differ in geographical distribution. *Comp. Biochem. Physiol. Part A Mol. Integr. Physiol.* **156**, 129-135.

Toledo, R. and Jared, C. (1993). Cutaneous adaptations to water balance in amphibians. *Comp. Biochem. Physiol. Part A Physiol.* **105**, 593-608.

Tracy, C. R., Reynolds, S. J., McArthur, L., Tracy, C. R. and Christian, K. A. (2007). Ecology of aestivation in a cocoon-forming frog, *Cyclorana australis* (Hylidae). *Copeia* **2007**, 901-912.

Tracy, C. R., Christian, K. A., Burnip, N., Austin, B. J., Cornall, A., Iglesias, S., Reynolds, S. J., Tixier, T. and Le Noene, C. (2013). Thermal and hydric implications of diurnal activity by a small tropical frog during the dry season. *Austral. Ecol.* **38**, 476-483.

Trenberth, K. E., Dai, A., Van Der Schrier, G., Jones, P. D., Barichivich, J., Briffa, K. R. and Sheffield, J. (2014). Global warming and changes in drought. *Nat. Clim. Change* **4**, 17.

Ukkola, A. M., De Kauwe, M. G., Roderick, M. L., Abramowitz, G. and Pitman, A. J. (2020). Robust future changes in meteorological drought in CMIP6 projections despite uncertainty in precipitation. *Geophys. Res. Lett.* **47**, e2020GL087820.

Walvoord, M. E. (2003). Cricket frogs maintain body hydration and temperature near levels allowing maximum jump performance. *Physiol. Biochem. Zool.* **76**, 825-835.

Wassens, S., Walcott, A., Wilson, A. and Freire, R. (2013). Frog breeding in rain-fed wetlands after a period of severe drought: implications for predicting the impacts of climate change. *Hydrobiologia* **708**, 69-80.

Williams, S. E., Shoo, L. P., Isaac, J. L., Hoffmann, A. A. and Langham, G. (2008). Towards an integrated framework for assessing the vulnerability of species to climate change. *PLoS Biol.* **6**, e325.

Withers, P. (1995). Cocoon formation and structure in the estivating Australian desert frogs, Neobatrachus and Cyclorana. *Aust. J. Zool.* **43**, 429-441.

Withers, P. C., Hillman, S. S. and Drewes, R. C. (1984). Evaporative water loss and skin lipids of anuran amphibians. *J. Exp. Zool.* **232**, 11-17.

Wu, N. C. and Seebacher, F. (2021). Bisphenols alter thermal responses and performance in zebrafish (*Danio rerio*). *Conserv. Physiol.* **9**, coaa138.

Wu, N. C. and Seebacher, F. (2022). Physiology can predict animal activity, exploration, and dispersal. *Comm. Biol.* **5**, 1-11.

Wygoda, M. (1988). Adaptive control of water loss resistance in an arboreal frog. *Herpetologica* **44**, 251-257.

Wygoda, M. L. (1984). Low cutaneous evaporative water loss in arboreal frogs. *Physiol. Zool.* **57**, 329-337.

Zhao, T. and Dai, A. (2022). CMIP6 model-projected hydroclimatic and drought changes and their causes in the twenty-first century. *Journal of Climate* **35**, 897-921.

Zylstra, E. R., Swann, D. E., Hossack, B. R., Muths, E. and Steidl, R. J. (2019). Drought-mediated extinction of an arid-land amphibian: insights from a spatially explicit dynamic occupancy model. *Ecol. Appl.* **29**, e01859.

FIGURES

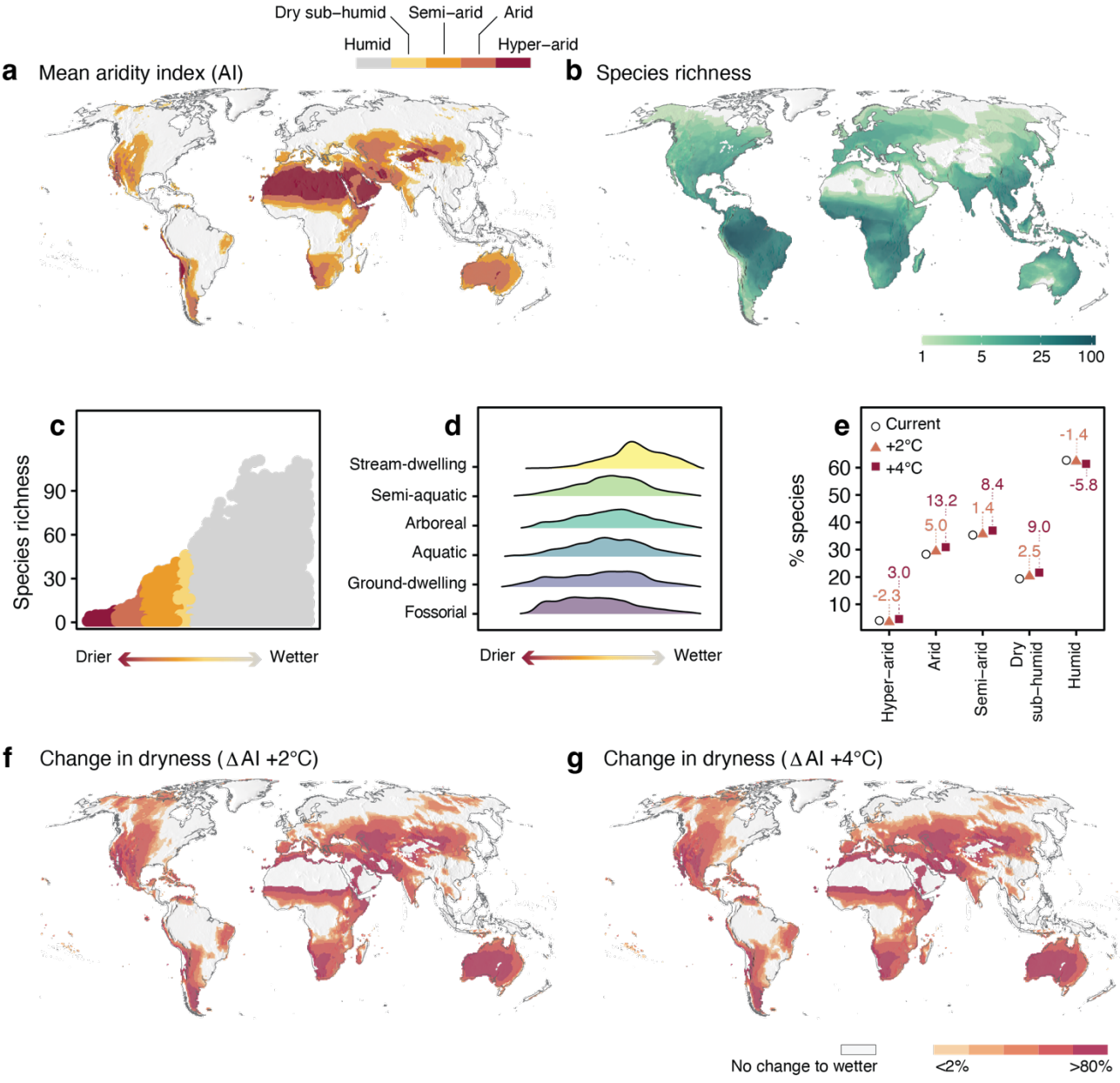

Figure 1. Relationship between the spatial distribution of anuran species and the degree of dryness of the climate. (a) The spatial distribution of the mean aridity index (AI) based on the precipitation and potential evapotranspiration between 1981–2010, and **(b)** is the anuran species richness based on the IUCN spatial assessment. **(c)** The relationship between mean AI and species richness, where the wetter the climate (lower aridity), the more species richness within the grid cell (0.5°) than drier climates. **(d)** Ecotype-specific distribution of anurans across AI, where stream-dwelling species tend to be conjugated in humid areas, while fossorial species tend to be found in drier areas. **(e)** Change in the percentage of species in each grid cell (0.5°) grouped by AI category between the current climate (yearly average from 1981–2010) and future warming scenario of +2°C

and +4°C by 2080–2099. Under a +2°C warming scenario, there will be a -1.4 % decrease in percentage of species occupying humid regions and a 6.6% increase in percentage of species occupying dry sub-humid to arid regions. Under a +4°C warming scenario, there will be a -5.8 % decrease in percentage of species occupying humid regions and a 33.5% increase in percentage of species occupying dry sub-humid to arid regions. **(f–g)** Spatial change in mean dryness (decrease in AI) under a +2°C and +4°C warming scenario.

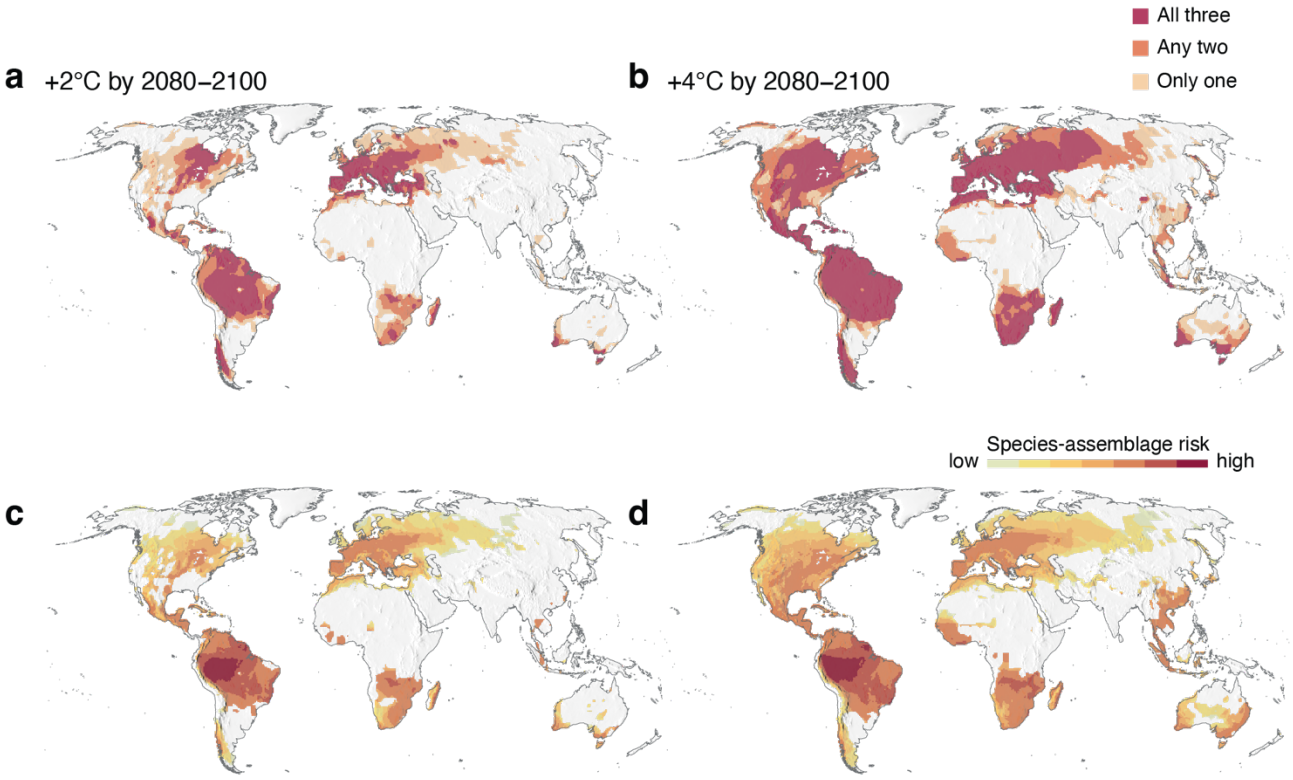

Figure 2. Assemblage-level risk due to multiple aspects of increasing drought events. Grid cells with anuran occurrences exposed to either a single metric (frequency, duration, or intensity: only one), any two metrics (frequency and intensity, frequency and duration, duration and intensity: any two), or all three metrics (frequency, duration, and intensity: all three) of extreme drought events beyond their historic levels by 2080–2100 under **(a)** a +2°C warming scenario (SSP2–4.5) and **(b)** a +4°C warming scenario (SSP5–8.5). The results for drought frequency, intensity, and duration alone were presented in the **Extended Data Figs. 1–3**. **(c–d)** Assemblage-level risk based on the number of drought risk by number of species per grid cell under **(c)** a +2°C warming scenario (SSP2–4.5) and **(d)** a +4°C warming scenario (SSP5–8.5). The drought risk was weighed by species assemblage, where a grid cell with high drought risk and high species richness has a higher risk score than a grid cell with high drought risk and low species richness.

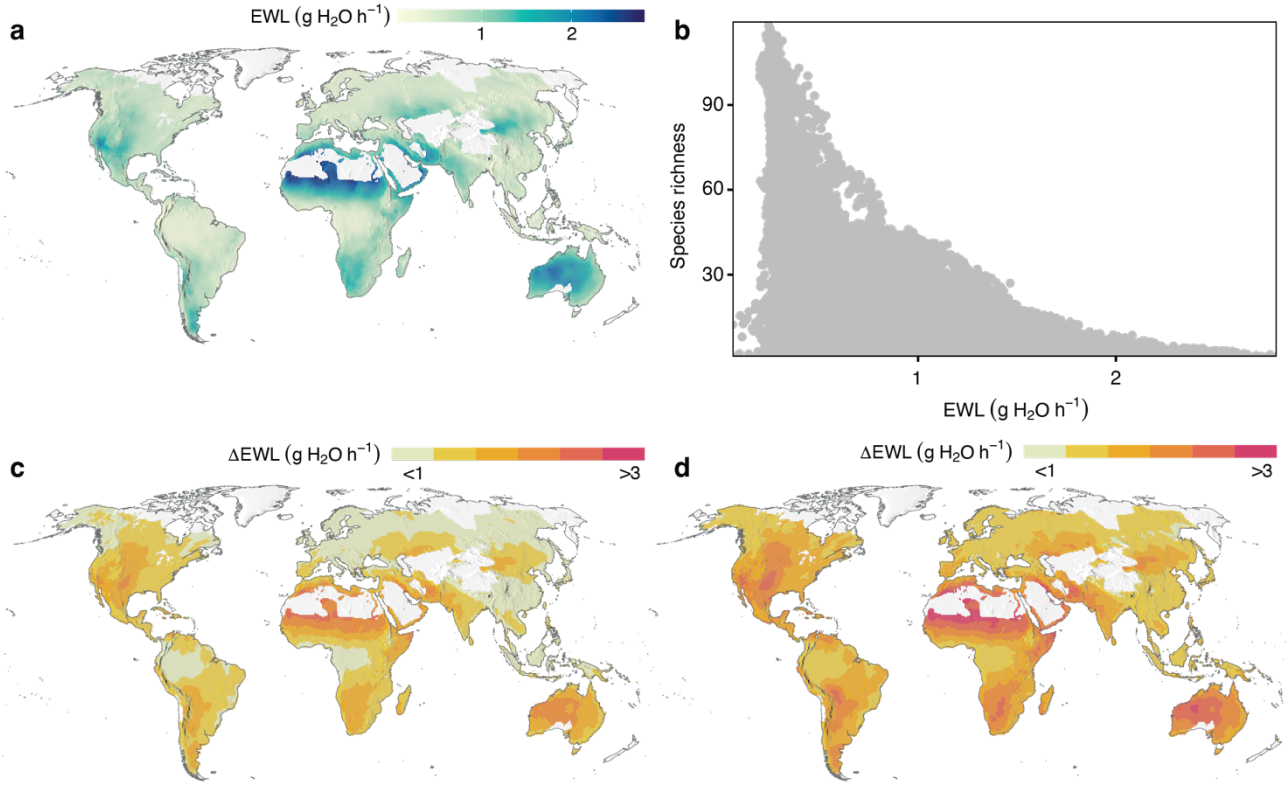

746

747 **Figure 3. Variation in evaporative water loss (EWL) for a typical 8.7 g frog**. **(a)** Spatial
748 variation in EWL (g H_2O h^{-1}) under the current (1981–2010) scenario. **(b)** Relationship between
749 EWL and species richness where the number of species tends to be higher in areas that provide low
750 EWL potential (Ecotype specific relationship is presented in **Supplementary Fig. S11**). Bottom
751 maps represent change in EWL (ΔEWL; g H_2O h^{-1}) under **(c)** a +2°C warming scenario (SSP2–4.5)
752 and **(d)** a +4°C warming scenario (SSP5–8.5).

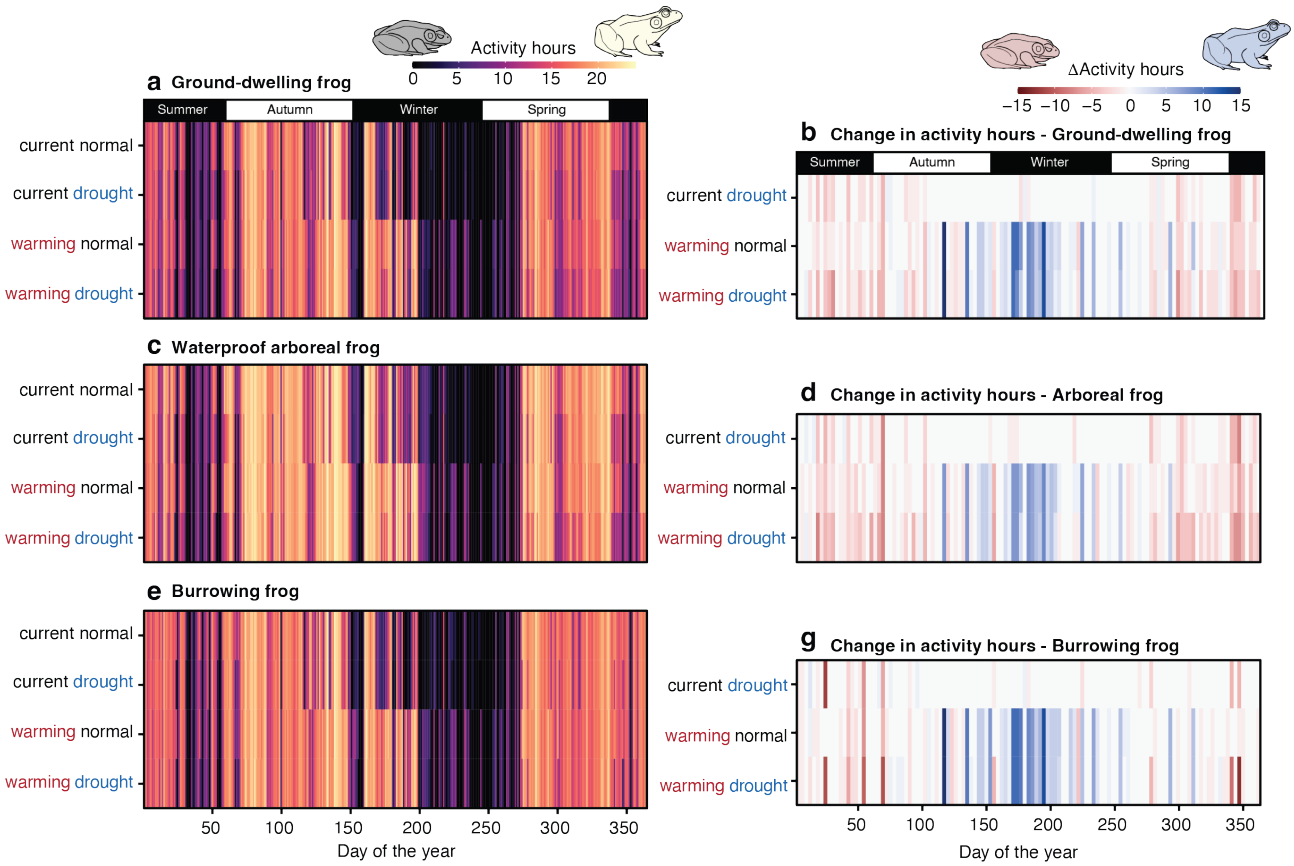

753

754 **Figure 4. Total hours for potential activity and change in activity under different climate**
755 **conditions for a hypothetical 8.7 g frog in Queensland, Australia.** Daily hours of potential
756 activity within suitable thermal and hydric conditions (left panels) and change in activity relative to
757 the current normal scenario (right panels) for **(a-b)** a ground-dwelling frog, (**c-d)** a water-proof
758 arboreal frog, and **(e-g)** a burrowing frog. Total potential activity represented as numbers presented
759 in Supplementary Table S6.

760

EXTENDED FIGURES

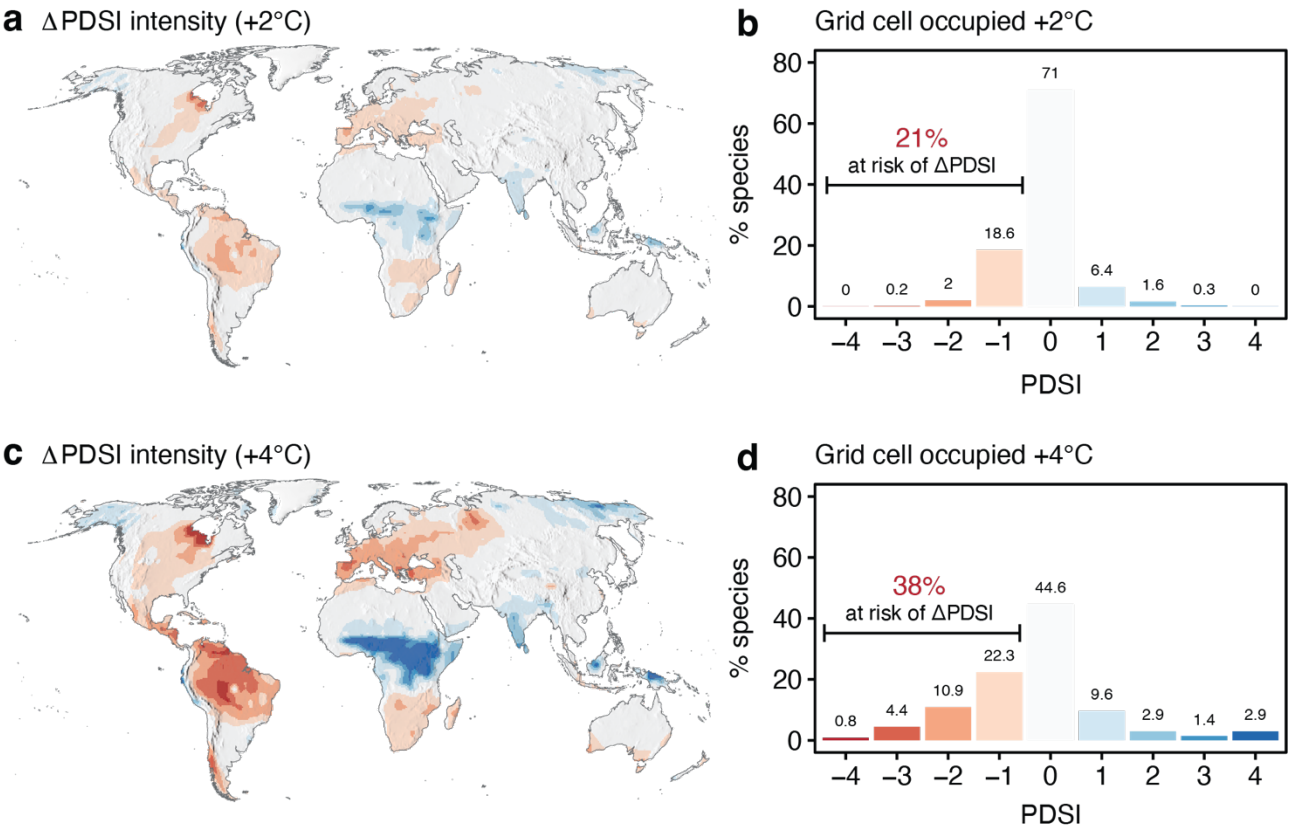

Extended Data Fig. 1 | Risk to increasing drought intensity for anurans by 2080–2100. (a) Change in the Palmer Drought Severity Index (ΔPDSI) under a +2°C warming scenario (Shared Socioeconomic Pathways 2–4.5; SPP2–4.5) by 2080–2100 relative to the current scenario (1970–1999). A decrease ΔPDSI indicates higher drought occurrences, while an increase ΔPDSI indicates more extreme wetness. **(b)** Percentage of anuran species occupancy in each PDSI category grid cell (0.5°) under a +2°C warming scenario, where 21% of species are in areas that are at risk of increasing drought. **(c)** Change in ΔPDSI under a +4°C warming scenario (SPP5–8.5). **(d)** Percentage of anuran species occupancy in each PDSI category grid cell (0.5°) under a +4°C warming scenario, where 38% of species are in areas that are at risk of increasing drought.

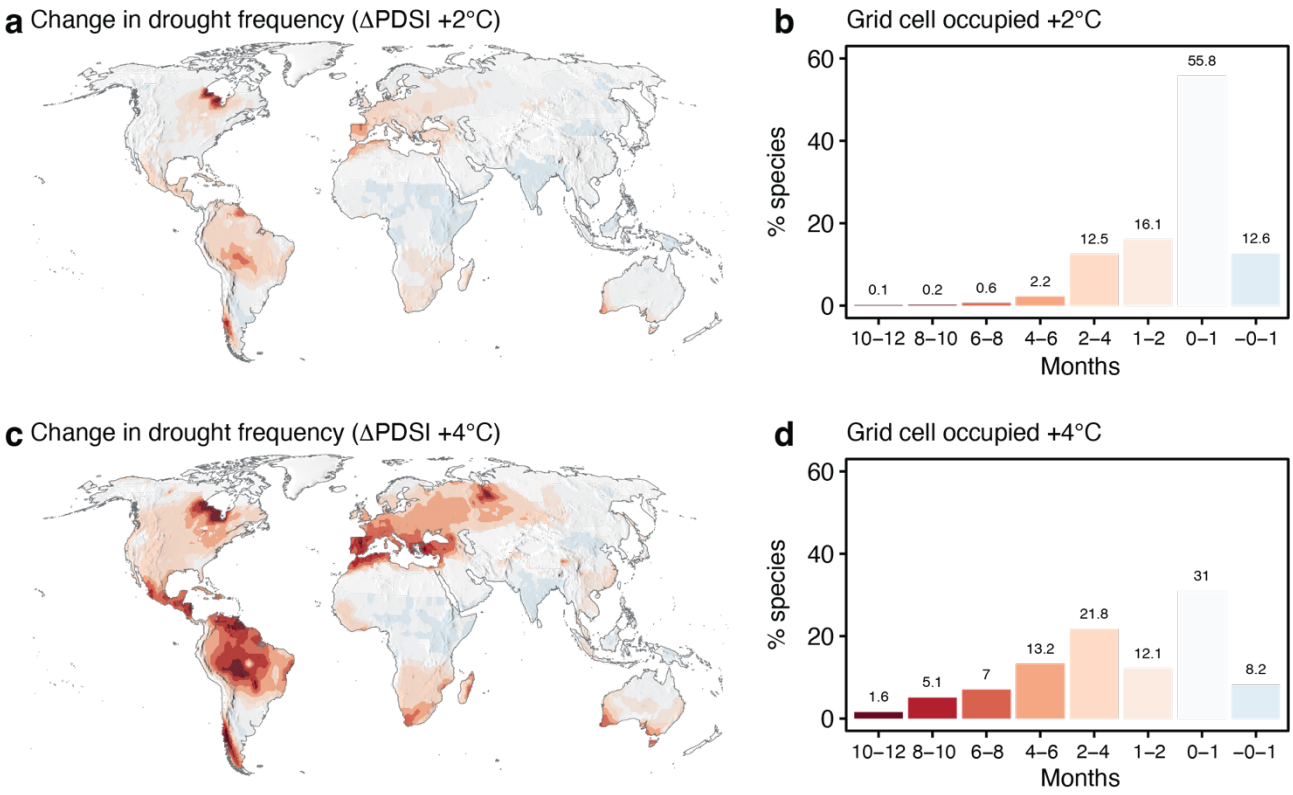

773

774 **Extended Data Fig. 2 | Risk to increasing drought frequency for anurans by 2080–2100. (a)**
775 Change in the Palmer Drought Severity Index frequency ($\Delta PDSI_{[frequency]}$) under a +2°C warming
776 scenario (Shared Socioeconomic Pathways 2–4.5; SPP2–4.5) by 2080–2100 relative to the current
777 scenario (1970–1999). $\Delta PDSI_{[frequency]}$ was defined as change in monthly drought below -2
778 (moderate to extreme drought) within a 20 year period. **(b)** Percentage of anuran species occupancy
779 in each frequency category grid cell (0.5°) under a +2°C warming scenario. **(c)** Change in the
780 $\Delta PDSI_{[frequency]}$ under a +4°C warming scenario **(**SPP5–8.5**). (d)** Percentage of anuran species
781 occupancy in each frequency category grid cell (0.5°) under a +4°C warming scenario.

782

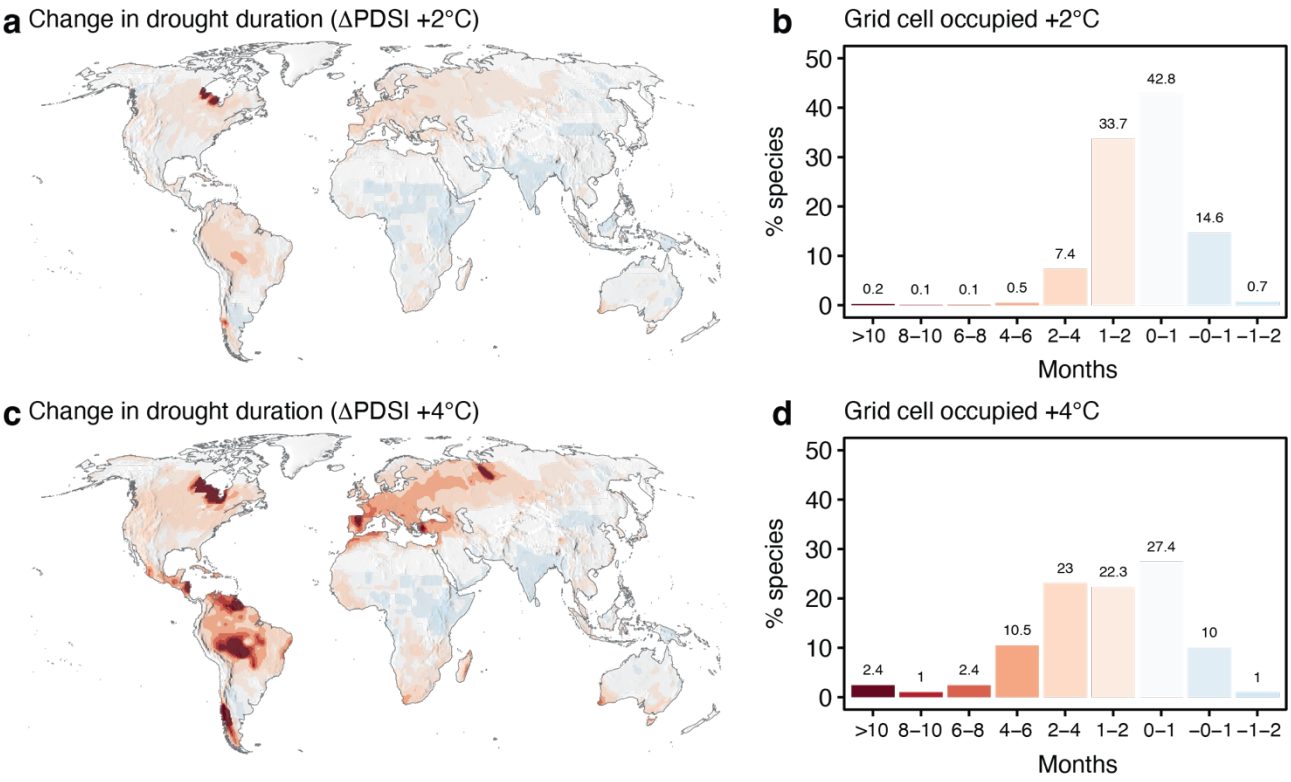

783

784 **Extended Data Fig. 3 | Risk to increasing drought duration for anurans by 2080–2100. (a)**
785 Change in the Palmer Drought Severity Index frequency ($\Delta PDSI_{[duration]}$) under a +2°C warming
786 scenario (Shared Socioeconomic Pathways 2–4.5; SPP2–4.5) by 2080–2100 relative to the current
787 scenario (1970–1999). $\Delta PDSI_{[duration]}$ was defined as consecutive months under moderate to extreme
788 drought (PDSI < -2) within a 20 year period. **(b)** Percentage of anuran species occupancy in each
789 duration category grid cell (0.5°) under a +2°C warming scenario. **(c)** Change in the $\Delta PDSI_{[duration]}$
790 under a +4°C warming scenario **(**SPP5–8.5**). (d)** Percentage of anuran species occupancy in each
791 duration category grid cell (0.5°) under a +4°C warming scenario.

792

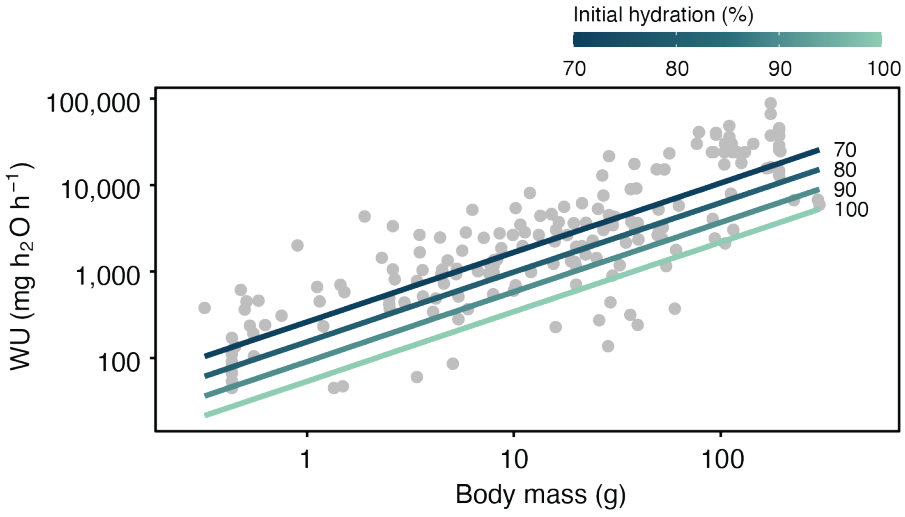

793

Extended Data Fig. 5 | Relationship between cutaneous water uptake with body mass of adult anurans. Gradient coloured lines represent the influence of initial hydration of the frog on the rate of water uptake. Individual data points represent mean water uptake measurements (n = 143).